

SILICON ISOTOPE RATIOS IN CAIS: IN-SITU LASER-ABLATION MC-ICPMS MEASUREMENTS AND COMPARISONS WITH MAGNESIUM ISOTOPE RATIOS.

A. Shahar¹ and E. D. Young^{1,2},
¹Department of Earth and Space Sciences, University of California Los Angeles, 595 Charles Young Dr. E., Los Angeles, CA 90095 (ashahar@ess.ucla.edu), ²Institute of Geophysics and Planetary Physics (eyoung@ess.ucla.edu).

Introduction: High-precision measurements of $^{25}\text{Mg}/^{24}\text{Mg}$ by multiple-collector inductively coupled plasma-source mass spectrometry (MC-ICPMS) have been used recently in our laboratory to constrain the thermal history of calcium aluminum-rich inclusions (CAIs) [1]. Presence of primary zoning profiles in at least some CAIs points to supersolidus and subsolidus diffusion as important factors in controlling isotope fractionation. Previous model calculations suggested that the details of the isotope selectivity of Mg isotope diffusion in igneous CAI melts may ultimately control the overall degree of heavy isotope enrichment during evaporation [2]. Our work suggests that subsequent heating in the solid state imposes modifications to the original isotopic signals [1]. We are looking for evidence for both processes in CAIs.

The importance of isotope fractionation during diffusion in CAI melts is illustrated with a finite difference model for Mg isotope fractionation of a CAI starting with a diameter of 0.3 cm held at liquidus temperature for 60 minutes (Fig. 1). The model shows enrichment in $\delta^{25}\text{Mg}$ only when proper account is made for the slight disparity in diffusivities between ^{25}Mg and ^{24}Mg . In this calculation we used $D(^{25}\text{Mg})=(24/25)^\beta D(^{24}\text{Mg})$ with $\beta=0.1$ as suggested by [3]. In contrast, when $\beta = 0$, isotope fractionation is

confined to a boundary layer and the degree of enrichment in the body of the object outside of the boundary layer is zero (Fig. 1).

Comparisons between Mg isotope ratios and Si isotope ratios should help constrain the role of diffusion in determining the isotopic composition of igneous CAIs. The β relating the diffusivities of the Si isotopes in melt, $D(^{29}\text{Si})$ and $D(^{28}\text{Si})$, is thought to be much smaller than the value for Mg (< 0.025 for Si compared with ~ 0.1 for Mg) [3]. Accordingly, one expects $\delta^{29}\text{Si}$ to be systematically lower than $\delta^{25}\text{Mg}$ in evaporated igneous CAIs (both relative to chondritic values) given the similar volatility of these elements. Bulk measurements give hints of this, but isotopic resetting during prolonged heating of CAIs makes interpretation of bulk properties uncertain [4]. Profiles of isotope ratios across the objects are needed to understand the extent of resetting.

Until now, detailed comparisons between Mg and Si isotope ratios within individual CAIs have proven difficult due to analytical uncertainties. Here we explore the use of ultraviolet laser ablation MC-ICPMS (UV LA-MC-ICPMS) as a tool for measuring $^{29}\text{Si}/^{28}\text{Si}$ and $^{30}\text{Si}/^{28}\text{Si}$ in CAIs.

LA-MC-ICPMS Method: In-situ Si isotope ratio analyses were measured using a 193 nm excimer laser (NewWave Research UP) coupled to a ThermoFinnigan Neptune MC-ICPMS at UCLA. Correction for instrumental mass bias was made using sample-standard bracketing. The standard was a sample of San Carlos olivine (SC olivine). The mass spectrometer was operated at a moderate mass resolving power of ~ 7500 (entrance slit of 30 μm , $2R = 812$ mm), permitting elimination of N_2^+ and NO^+ interferences on $m/z = 28$ and 30, respectively, while minimizing signal losses. A preliminary investigation of the effects of $^{56}\text{Fe}^{++}$ and $^{58}\text{Fe}^{++}$ (not a factor for most CAI analyses) was undertaken with solutions. We could detect no measurable $m/z = 28$ in a 5 ppm Fe solution in weak HNO_3 acid. Silicon isotope ratios measured on 3ppm Si in the presence of 0.1, 0.3, and 1 ppm Fe showed no departures from mass dependent fractionation in $^{29}\text{Si}/^{28}\text{Si}$ and $^{30}\text{Si}/^{28}\text{Si}$. On-peak blanks were measured before each analysis to correct for 0.4%, 3%, and 3% backgrounds on $m/z = 28, 29,$ and 30, respectively. Laser spot size was 100 μm to 150 μm depending

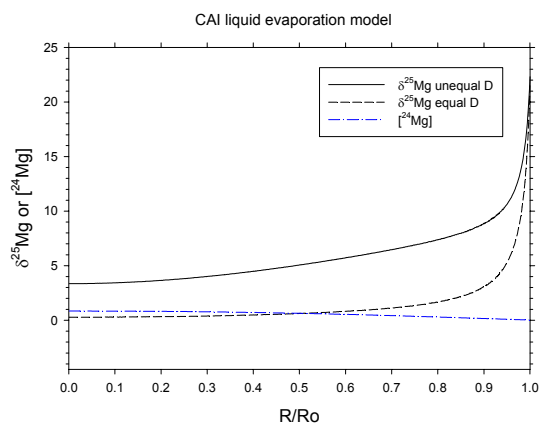


Fig. 1. Model calculation showing changes in $\delta^{25}\text{Mg}$ and Mg concentration [Mg] after 60 minutes for a molten CAI 0.3 cm in diameter prior to evaporation. The vapor/liquid Mg partition coefficient is 50 and dr/dt is -1.0×10^{-5} cm/s. R/R_0 is the normalized radius of the shrinking object.

upon the material. The laser was operated at an ultra-violet fluence of $\sim 25 \text{ J/cm}^2$ and a pulse repetition rate of 2 to 4 Hz.

Description of CAI Allende 3576-1 b: Allende 3576-1 b is an irregular type B1 CAI measuring 4 mm in length and 3.5 mm in width. It is composed mainly of intergrown melilite and Ti-Al-rich diopside +/- spinel surrounded by a mantle of melilite. Melilite $\text{Al}_2\text{Mg}_{-1}\text{Si}_{-1}$ increases towards the edge of the object. The Mg isotopic composition of this object was studied previously by LA-MC-ICPMS. Results, presented at the last LPSC meeting [1], show that $\delta^{25}\text{Mg}$ decreases towards the margin of the object (Fig. 2). Simon et al. [5] show that the change in Mg isotope ratios from core to rim of the object is best explained by near-solidus, solid-state diffusive equilibration with a chondritic Mg-bearing gas on a cumulative time scale of ca. 300 yrs (Fig. 2), a history that coincides

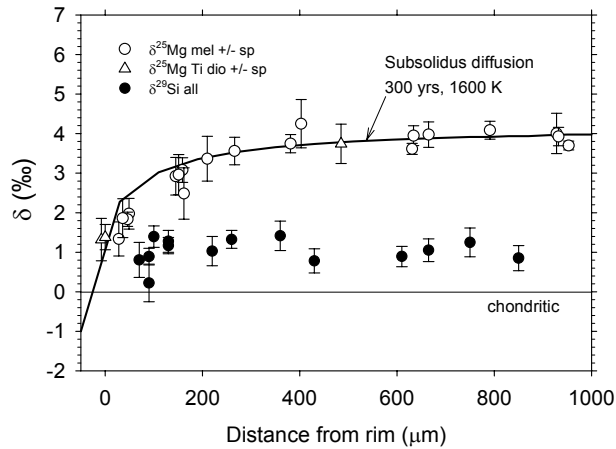


Fig. 2. Plot of $\delta^{25}\text{Mg}$ (open symbols) and $\delta^{29}\text{Si}$ (closed symbols) for CAI Allende 3576-1 b. The Mg isotope data are fit by subsolidus diffusion of Mg at the outer boundary of the object. The source of Mg is gas with canonical solar nebular partial pressure and $\delta^{25}\text{Mg} = 0$. The profile is fit using a cumulative time scale of 300 (+/- 20) yrs. The $\delta^{29}\text{Si}$ data are lower and show a hint of depletion at the margin.

with that required to reset the apparent initial $^{26}\text{Al}/^{27}\text{Al}$ in many CAIs to canonical values [4]. This diffusive resetting postdates the original evaporation processes that gave rise to the $\delta^{25}\text{Mg}$ values of about 4 ‰ relative to chondritic observed in the interior of the CAI (Fig. 2).

Si Isotope Results: In-situ analyses of $\delta^{29}\text{Si}$ and $\delta^{30}\text{Si}$ relative to SC olivine exhibit a precision of about +/- 0.2 per mil 1σ . In all cases analyses are within 2s of mass-dependent fractionation (Fig. 3). The $\delta^{29}\text{Si}$

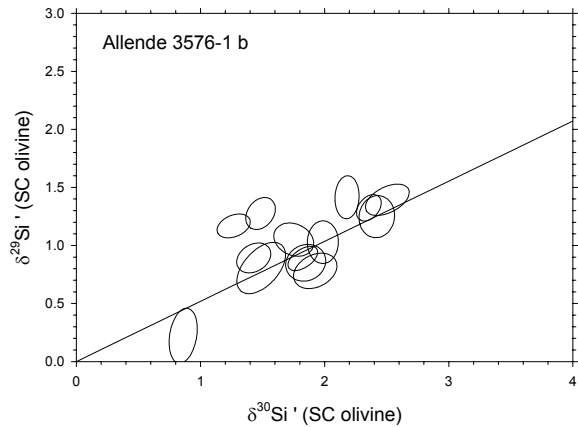


Fig. 3. Plot of $\delta^{29}\text{Si}$ vs. $\delta^{30}\text{Si}$ for CAI Allende 3576-1 b obtained by LA-MC-ICPMS. Error ellipses represent 1σ internal precision.

values are substantially lower than $\delta^{25}\text{Mg}$ (Fig. 2). There is a hint of decreasing $\delta^{29}\text{Si}$ at the margin of the object, sympathetic to the decrease in $\delta^{25}\text{Mg}$, but higher spatial resolution will be required to investigate this feature (higher spatial resolution will be achieved using patterned ablation).

The difference between $\delta^{29}\text{Si}$ and $\delta^{25}\text{Mg}$ is indicative of the expected lower β for Si than for Mg, and is broadly consistent with earlier bulk measurements [6].

Conclusion: In-situ $^{29}\text{Si}/^{28}\text{Si}$ and $^{30}\text{Si}/^{28}\text{Si}$ analyses can be obtained using LA-MC-ICPMS with useful precision comparable to that for Mg isotope ratios. Analyses for a type B1 CAI from Allende show markedly lower $\delta^{29}\text{Si}$ than $\delta^{25}\text{Mg}$, an observation that should be useful in constraining the role of isotope selective diffusion in CAI melts through the β parameter in the relation $D(m_2)/D(m_1) = (m_1/m_2)^\beta$, where m_i is the atomic mass and D is the diffusivity in melt for the indicated mass. The fact that $0 < \delta^{29}\text{Si} < \delta^{25}\text{Mg}$ in the interior of the object means that for Si $0 < \beta < 0.1$, as suggested by previous calculations for Si and measurements of Ge isotope fractionation with diffusion [3].

References: [1] Simon J. I. et al. (2005) *Lunar and Planetary Science Conference XXXVI*, Abstract 2068. [2] Richter F. M. (2004) *Geochimica et Cosmochimica Acta*, 68, 4971-4992. [3] Richter F. M. et al. (2003) *Geochimica et Cosmochimica Acta*, 67, 3905-3923. [4] Young E. D. et al. (2005) *Science*, 308, 223-227. [5] Simon J. et al. (2006) *LPSC 2006*. [6] Clayton R. N. et al. (1988) *Philosophical Transactions of the Royal Society of London*, A 325, 483-501.